

Numerical study of instabilities driven by the energetic neutral beam ions in NSTX

E. V. Belova, N. N. Gorelenkov, C. Z. Cheng,
R. C. Davidson, E. D. Fredrickson (PPPL)

Outline

- Motivation, experimental observations of sub-cyclotron frequency modes in NSTX
- Numerical model, delta-f method
- Self-consistent equilibrium calculations including energetic ions
- Linear delta-f simulations; GAE and CAE modes
- Summary and future work

Motivation

- Sub-cyclotron frequency modes are observed in NSTX. Experimental observations and analytic calculations¹ suggest that these are excited by **energetic neutral beam ions** during NBI injection.
- Modes are predicted to be driven unstable through cyclotron resonance with beam ions.
- Strong anisotropy in the fast-ion pitch-angle distribution provides the energy source for CAE and GAE instabilities.
- CAEs may be responsible for the **enhanced energy transfer**² from the fast ions to the thermal ions.
- Numerical simulations are needed to include: self-consistent anisotropic equilibrium, FLR effects, thermal ion and nonlinear effects.

[1] N. N. Gorelenkov and C. Z. Cheng, Nucl. Fusion 35 1743 (1995); [2] D. Gates et al. PRL 2001

Nonlinear 3D **HYM** (Hybrid and MHD) global simulation code

- 2d order accurate in time, explicit scheme
- 4th order spatial derivatives (3D finite difference)
- Linearized or nonlinear
 - MHD
 - MHD + fast ions
 - Hybrid (fluid electrons, particle ions)
- For particles: delta-f scheme
- FRC or ST equilibrium

Self-consistent MHD + fast ions coupling scheme

Background plasma - fluid:

$$\rho \frac{d\mathbf{V}}{dt} = -\nabla p + (\mathbf{j} - \mathbf{j}_i) \times \mathbf{B} - n_i (\mathbf{E} - \eta \mathbf{j})$$

$$\mathbf{E} = -\mathbf{V} \times \mathbf{B} + \eta \mathbf{j}$$

$$\mathbf{B} = \mathbf{B}_0 + \nabla \times \mathbf{A}$$

$$\partial \mathbf{A} / \partial t = -\mathbf{E}$$

$$\mathbf{j} = \nabla \times \mathbf{B}$$

$$\partial p^{1/\gamma} / \partial t = -\nabla \cdot (\mathbf{V} p^{1/\gamma})$$

$$\partial \rho / \partial t = -\nabla \cdot (\mathbf{V} \rho)$$

Fast ions – delta-F scheme:

$$\frac{d\mathbf{x}}{dt} = \mathbf{v}$$

$$\frac{d\mathbf{v}}{dt} = \mathbf{E} - \eta \mathbf{j} + \mathbf{v} \times \mathbf{B}$$

$$w = \delta F / F \quad - \text{particle weight}$$

$$\frac{dw}{dt} = -(1-w) \frac{d(\ln F_0)}{dt}$$

$$F_0 = F_0(\varepsilon, \mu, p_\phi)$$

ρ , \mathbf{V} and p are bulk plasma density, velocity and pressure, n_i and \mathbf{j}_i are fast ion density and current, $n_i \ll n$ – is assumed.

Equilibrium with energetic ions

Grad-Shafranov equation for two-component plasma: MHD plasma (bulk) and fast ions

$$\frac{\partial^2 \psi}{\partial z^2} + R \frac{\partial}{\partial R} \left(\frac{1}{R} \frac{\partial \psi}{\partial R} \right) = -R^2 p' - HH' - GH' + RJ_{i\phi}$$

where $\mathbf{B} = \nabla \phi \times \nabla \psi + h \nabla \phi$

$$h(R, z) = H(\psi) + G(R, z)$$

$$\mathbf{J}_{ip} = \nabla G \times \nabla \phi$$

$\mathbf{J}_{ip}, J_{i\phi}$ - poloidal and toroidal fast ion current, $p(\psi)$ - bulk plasma pressure, G - poloidal stream function.

Equilibrium calculations

Equilibrium distribution function $F_0 = F_1(v)F_2(\lambda)F_3(p_\phi)$

$$\left(\begin{array}{l} F_1(v) = \frac{1}{v^3 + v_*^3}, \quad \text{for } v < v_0 \\ F_2(\lambda) = \exp(-(\lambda - \lambda_0)^2 / \Delta\lambda^2) \\ F_3(p_\phi) = \frac{(p_\phi - p_0)^\beta}{(R_0 v - \psi_0 - p_0)^\beta}, \quad \text{for } p_\phi > p_0 \end{array} \right.$$

where $v_0 \approx 3v_A$, $v_* = v_0/\sqrt{3}$, $\lambda = \mu B_0/\varepsilon$ - pitch angle,
 $\lambda_0 = 0.8 - 1$,

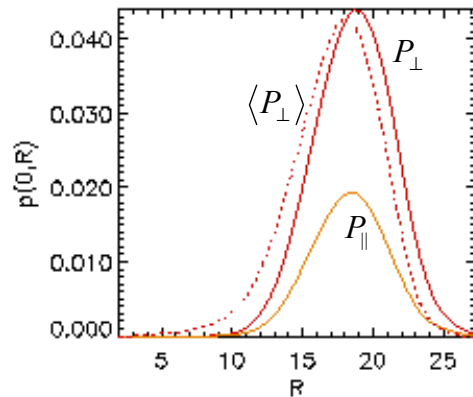
and $\mu = \mu_0 + \mu_1$ includes first-order corrections [Littlejohn'81]:

$$\mu = \frac{(\mathbf{v}_\perp - \mathbf{v}_d)^2}{2B} - \frac{\mu_0 v_\parallel}{2B} [\hat{\mathbf{b}} \cdot \nabla \times \hat{\mathbf{b}} - 2(\hat{\mathbf{a}} \cdot \nabla \hat{\mathbf{b}}) \cdot \hat{\mathbf{c}}]$$

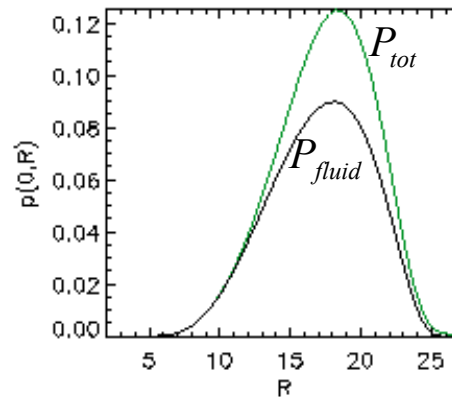
\mathbf{v}_d is magnetic gradient and curvature drift velocity, $\hat{\mathbf{c}} = \mathbf{v}_\perp/v_\perp$,
 $\hat{\mathbf{a}} = \hat{\mathbf{b}} \times \hat{\mathbf{c}}$

Equilibrium profiles of fluid and beam ion pressure

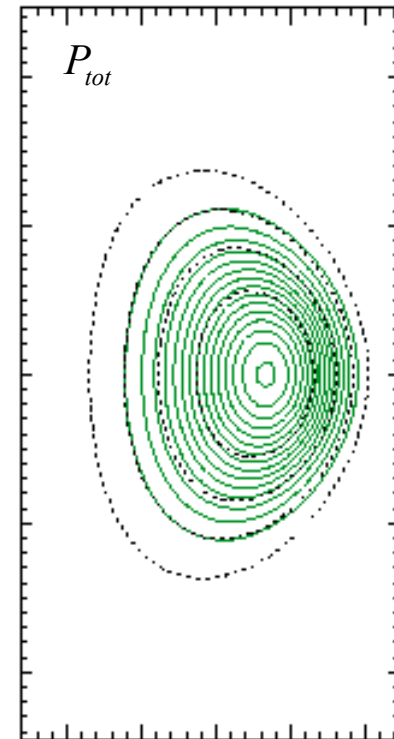
Beam ion density=3%, E=80keV;
Max thermal plasma beta=18%



Radial profiles of beam ion parallel and perpendicular pressure.

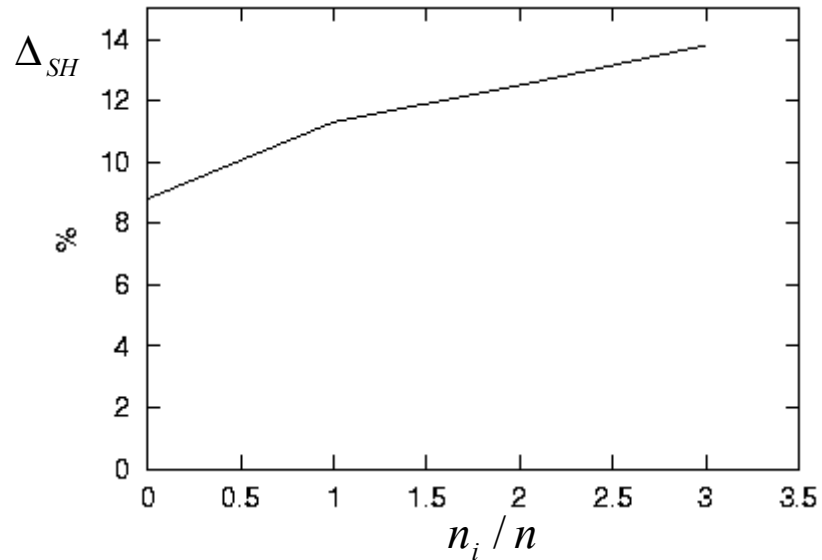
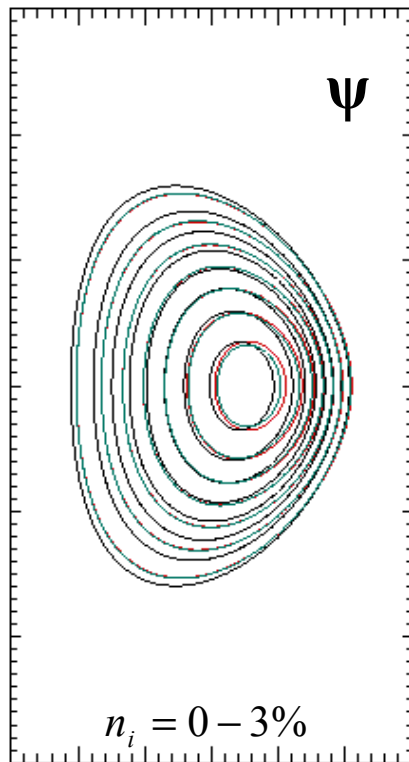


Radial profiles of total and fluid pressure.



Equilibrium with fast ions

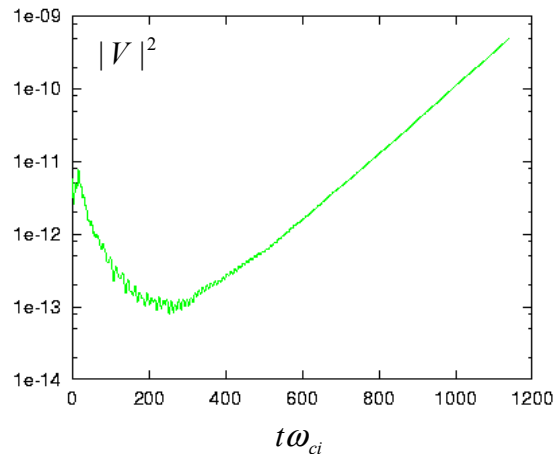
Effect of beam ions on equilibrium profiles for $V_0 = 3.4V_A$,
and different beam ion density.



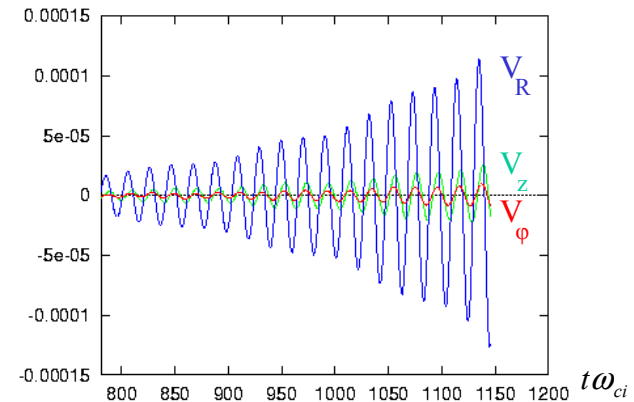
G-S iterations are done keeping total toroidal current and maximum bulk pressure the same: $I = \text{const}$, $\max(P) = 9\%$.

Linearized delta-f simulations

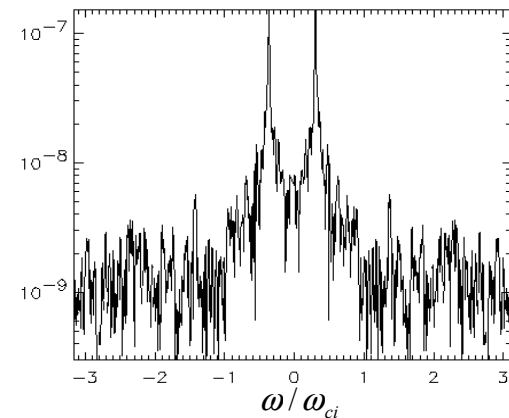
Simulations show instability for $n=4$
with $\gamma = 0.005\omega_{ci}$ and $\omega = 0.3\omega_{ci}$
for 3% beam ion density and $E=80\text{keV}$



Time evolution of bulk fluid kinetic energy for $n=4$.

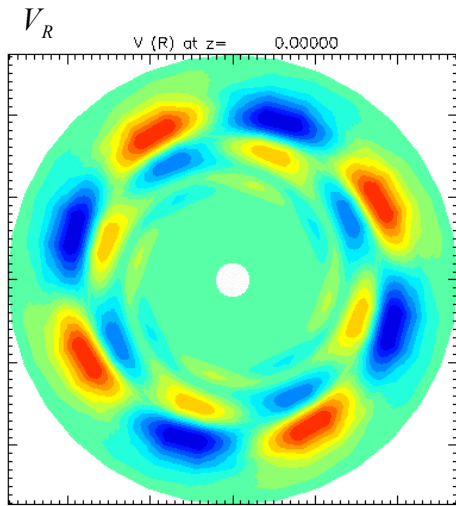


Fluid velocity at equatorial plane, $R=1.2R_0$

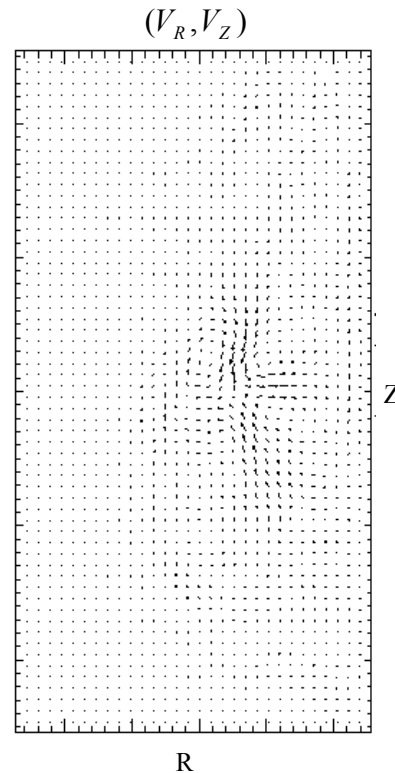


Frequency spectrum calculated from perturbed beam ion density.

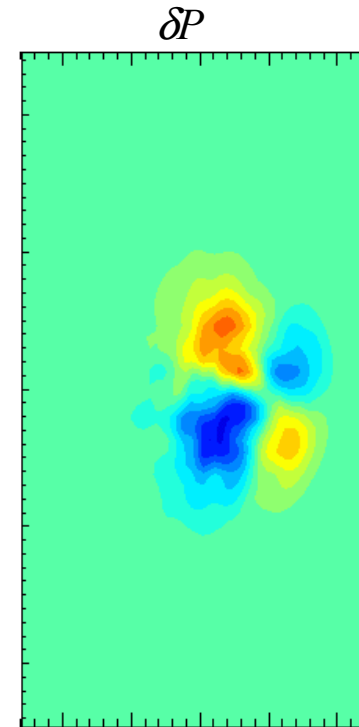
Linear mode structure (fluid velocity and pressure)



Contour plot of radial component of fluid velocity at equatorial plane.



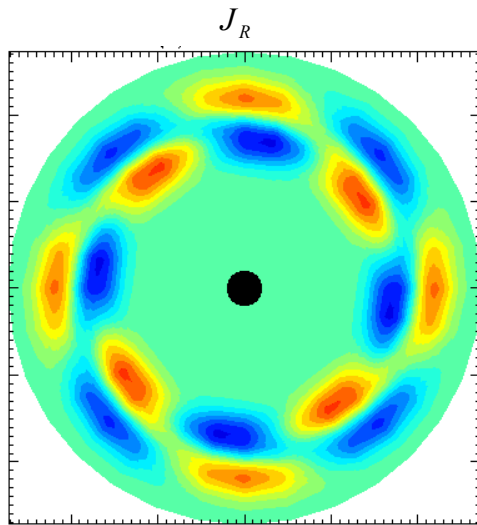
Vector plot of poloidal fluid velocity.



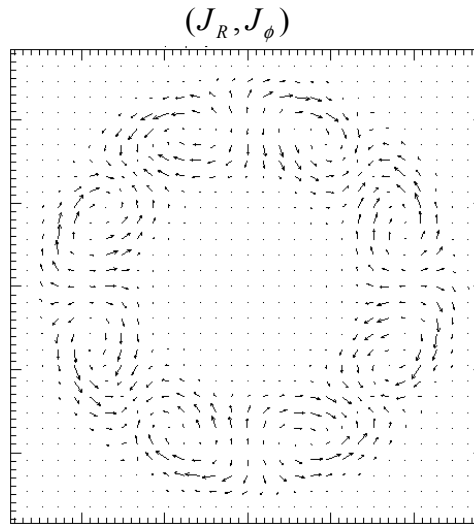
Contour plot of perturbed fluid pressure in poloidal plane.

Mode has a character of **Global Alfvén Eigenmode (GAE)** with $n=4$, $m=2$. It has large k_{\parallel} , and significant compressional component: $\delta B_{\parallel} \approx \frac{1}{3} \delta B_{\perp}$

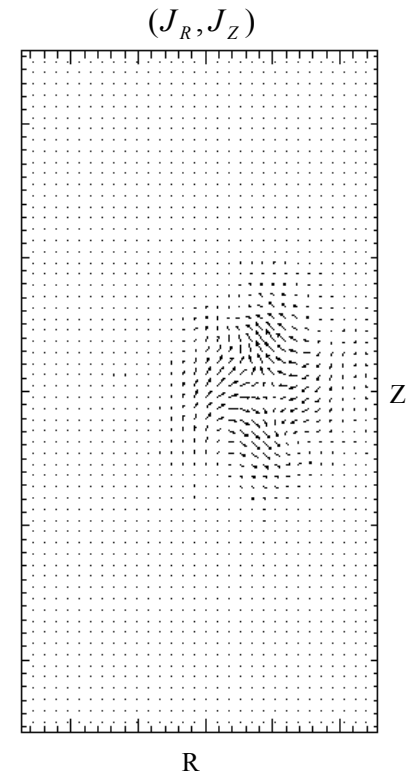
Linear mode structure (beam ion current)



Contour plot of radial component of perturbed beam ion current at equatorial plane.



Vector plot of beam ion current at equatorial plane.



Vector plot of poloidal beam ion current.

At low n , most unstable modes have a character of **GAE** modes

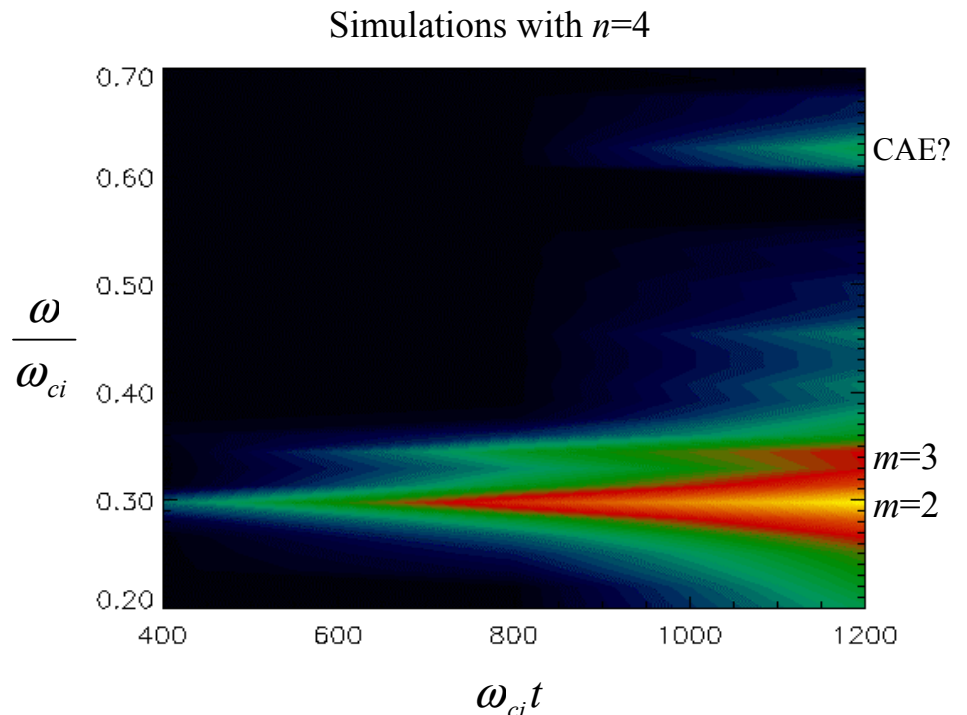
- Modes with $2 < n < 7$ are unstable.
- For each n , several m are unstable with large k_{\parallel} and $nm < 0$.
- Localized near magnetic axis.
- Large δB_{\perp} component.

- observed features agree with that of GAE mode, which exists just below the lower edge of the Alfvén continuum [Appert et al., 1982].

Resonant beam ions satisfy condition:

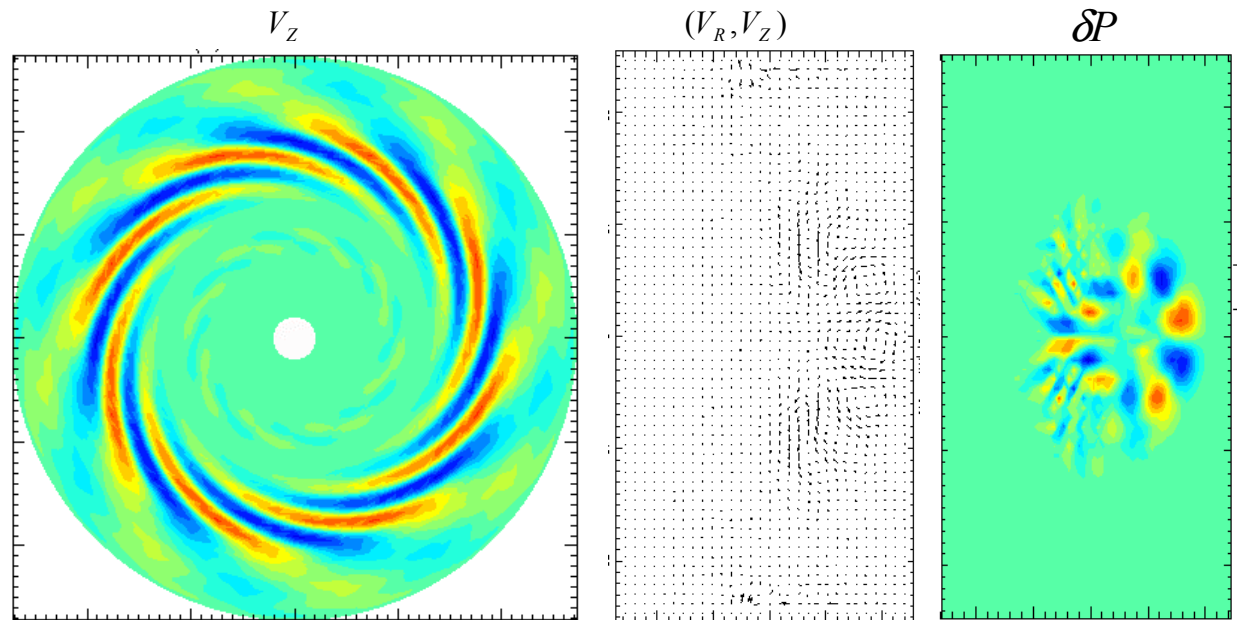
$$\omega - k_{\parallel} V_{\parallel} - \omega_{ci} = 0$$

Preliminary nonlinear results show saturation of instability at amplitudes: $\delta B \approx 10^{-4} - 10^{-3} B_0$



Simulations for $n > 7$ show localized modes with large compressional component (CAE?)

Hybrid simulation with $n=8$ show weakly unstable mode with $m=8-10$, $\omega = 0.4\omega_{ci}$, $\gamma \approx 0.001\omega_{ci}$, and $\delta B_{\parallel} > \delta B_{\perp}$

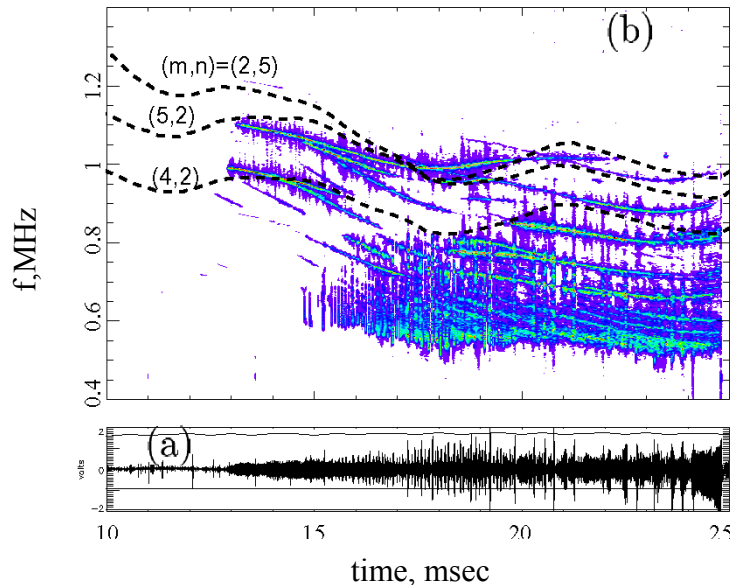


Contour plot of z-component of fluid velocity at equatorial plane

Vector plot of poloidal fluid velocity.

Contour plot of perturbed pressure.

Numerical simulations agree with observations and theory



Time evolution of the Mirnov signal (a), and its frequency spectrum (b) in NSTX shot #108236 [N. Gorelenkov, IAEA-2002].

- New observations of sub-cyclotron frequency modes during NBI injection show the spectrum line intersections, corresponding to **GAE** dispersion (with q-profile relaxation).
- Both CAE and GAE modes are observed.
- Theory predicts stronger instability for GAE with $\gamma/\omega \sim 1\%$ for $n_b \sim 1\%$ - in agreement with HYM simulations.

Summary

- Nonlinear 3D hybrid and MHD (FRC simulation) code has been modified for ST geometry – **HYM** code.
- Grad-Shafranov solver for general case of the two component plasma: MHD plasma with $p=p(\psi)$, plus energetic ions with anisotropic distribution.
- Simulations show that for large injection velocities, and strong anisotropy in the pitch-angle distribution, many Alfvén modes can be excited:
 - **GAE** modes for $2 < n < 7$ with $\gamma \approx 0.002 - 0.01\omega_{ci}$ and $\omega_r \approx 0.3 - 0.4\omega_{ci}$
 - for larger n , localized modes with smaller growth rate and large compressional component (**CAE?**)

Plans: simulations of GAE and CAE instabilities with:

- various fast particle distributions
- model electron Landau damping effects
- nonlinear effects and thermal ion effects